

Spectral properties of the ρ meson in a magnetic fieldSnigdha Ghosh,^{1,3,*} Arghya Mukherjee,^{2,3,†} Mahatsab Mandal,^{2,3,‡} Sourav Sarkar,^{1,3,§} and Pradip Roy^{2,3,||}¹Variable Energy Cyclotron Centre, 1/AF Bidhannagar, Kolkata 700 064, India²Saha Institute of Nuclear Physics, 1/AF Bidhannagar, Kolkata 700064, India³Homi Bhabha National Institute, Training School Complex, Anushaktinagar, Mumbai-400085, India

(Received 29 August 2016; revised manuscript received 8 November 2016; published 28 November 2016)

We calculate the rho meson mass in a weak magnetic field using effective $\rho\pi\pi$ interaction. It is seen that both ρ^0 and ρ^\pm masses decrease with the magnetic field in vacuum. The ρ meson dispersion relation has been calculated and shown to be different for ρ^0 and ρ^\pm . We also calculate the $\rho\pi\pi$ decay width and spectral functions of ρ^0 and ρ^\pm . The width is seen to decrease with eB and the spectral functions become narrower.

DOI: 10.1103/PhysRevD.94.094043

I. INTRODUCTION

Quantum chromodynamics (QCD) in the presence of a magnetic field has gained a lot of research interest in recent years. Apart from being exciting for its own intricacy and subtleties, the underlying physics of this strongly interacting matter under extreme conditions is enriched with many remarkable effects [1] like chiral magnetic effect [2–4], magnetic catalysis [5] as well as inverse magnetic catalysis effect [6], superconductivity of vacuum [7–9] and many more. It is also a remarkable fact that noncentral heavy ion collisions at RHIC and LHC do have the potential to provide the platform for their experimental verifications. In a noncentral heavy-ion collision at LHC, magnetic fields of the order $eB \sim 15m_\pi^2$ ($B \sim 5 \times 10^{15}$ Tesla) can be achieved [10] which is, in fact, higher than the typical QCD scale i.e. $eB \sim m_\pi^2$. Though in heavy-ion experiments, the fields are produced for a very short interval of time, they are good enough to substantially affect the strongly interacting fireball. Moreover, in case of a weak magnetic field limit the situation becomes almost analogous to the magnetic fields present inside magnetars which can be as high as $eB \sim 1 \text{ MeV}^2$ [11]. It is to be noted that the word “weak” is used to emphasize the dominance of QCD scale over the eB scale. Thus systematic understanding of strong interaction with a weak magnetic field background can also have significant applications in physics of neutron stars [12–16] as well as some other topics of cosmology and the early Universe. In this context we briefly recall the proceedings in one of the aforementioned effects, namely magnetic field induced superconductivity of vacuum.

Though the existence of a vacuum superconductor was first proposed a few years ago in Ref. [8] with pointlike vector mesons, recent researches considering internal

(quark) structures of the mesons kept on throwing new insights into this emerging phenomena. In Ref. [8] it was shown that nonminimal coupling of ρ mesons to the electromagnetic field could result in magnetic-field-induced superconductivity of the cold vacuum along the magnetic field direction. But due to the Vafa-Witten theorem [17] and QCD inequalities, Hidaka and Yamamoto concluded in Ref. [18] that QCD vacuum structure cannot be changed only by a magnetic field, i.e. magnetic-field-induced charged vector meson condensation is impossible. Soon after their work it has been argued in Ref. [19] that ρ^\pm condensation in a magnetic field background is consistent with the Vafa-Witten theorem because of the existence of a Higgs-like mechanism and was supported a year later in Ref. [20] where it was pointed out that the stronger version of the theorem [18] was plagued with the prejudiced choice of a generating functional on symmetric vacuum ignoring the other possibilities of nonsymmetric vacua. However, the authors of Ref. [18] also performed lattice QCD calculation in support of their conclusions. An interesting comment about that can be found in Ref. [21] where it was argued that although the results of Ref. [18] based on quenched lattice QCD simulation show a vanishing correlation in the large volume limit still that cannot be a reason to conclude against condensation because of the inherent inhomogeneous nature of the condensate. For example, Fig. 4 of Ref. [21] clearly demonstrates the fact that the vanishing of mass at the transition point depends on the order of the phase transition. In a careful investigation in the framework of the SU(2) Nambu-Jona-Lasinio (NJL) model Liu *et al.* [22] had pointed out that as the estimated critical field for charged ρ meson condensation is not strong enough, one needs to take into account the contributions of higher Landau levels as well, considering which the masses of charged ρ mesons with $S_z = 1$ and $S_z = -1$ do vanish at $eB_c \sim 0.2 \text{ GeV}^2$. However, in a very recent work in the hidden local symmetry approach in a constant magnetic field [23], it has been found that $\mathcal{O}(eB)^2$ corrections which

*snigdha.physics@gmail.com

†arghya.mukherjee@saha.ac.in

‡mahatsab@gmail.com

§sourav@vecc.gov.in

||pradipk.roy@saha.ac.in

are arising from the considerations of $\mathcal{O}(p^6)$ terms of derivative/chiral expansion, can in fact, change the trend of the effective mass from a decreasing to an increasing one resulting in the absence of any massless limit point. Thus it is obvious that a unanimous agreement on the existence of vacuum superconductor demands more research work in this field. In a recent work, the pion mass and dispersion relations have been calculated in [24] with nonzero eB in vacuum using an effective Lagrangian (with pseudoscalar as well as pseudovector pion-nucleon interactions). There it was shown that, for pseudoscalar coupling pion effective mass significantly decreases with weak external magnetic field. However, for pseudovector coupling, only a modest increase was reported. Using the same methodology, we, in this work, investigate the problem of ρ meson condensation with a phenomenological Lagrangian under the influence of a constant weak magnetic field in vacuum. The modification of dispersion relations due to finite temperature effects will be reported in our future work [25].

The paper is organized as follows. In Sec. II we discuss the formalism for calculating ρ meson self-energy in the presence of a weak magnetic field. Following similar approaches as in Ref. [24], we first define the scalar field Feynman propagators in constant external Abelian gauge field [26] by Schwinger's proper time formalism [27] and then calculate the effective mass up to one-loop order in self-energy. The results of our calculation are presented in Sec. III in which the effective mass variations with weak external field are presented followed by the dispersion relations. Finally in Sec. IV we conclude with a brief summary and discussions.

II. FORMALISM

The self-energy resummed ρ meson propagator satisfies the Dyson-Schwinger equation,

$$iD_{\mu\nu}(k) = iD_{\mu\nu}^0(k) + iD_{\mu\lambda}^0(k)(-i\Pi_{\rho}^{\lambda\sigma}(k))iD_{\sigma\nu}(k) \\ (D_{\mu\nu})^{-1} = (D_{\mu\nu}^0)^{-1} - \Pi_{\mu\nu}, \quad (1)$$

where the bare propagator for the massive vector field is given by

$$iD_{\mu\nu}^0 = \frac{-i}{k^2 - m_\rho^2 + i\epsilon} \left(g^{\mu\nu} - \frac{k^\mu k^\nu}{m_\rho^2} \right). \quad (2)$$

The pole of the effective propagator leads to the following dispersion relation:

$$\det[-(k^2 - m_\rho^2)g^{\mu\nu} + k^\mu k^\nu - \Pi_{\rho}^{\mu\nu}] = 0. \quad (3)$$

The exact form of the propagator of a charged scalar particle with mass m and charge e in the presence of a constant magnetic field can be written as [26,27]

$$D_B(x', x'') = \phi(x', x'') \int \frac{d^4 p}{(2\pi)^4} e^{-ip \cdot (x' - x'')} D_B(p), \quad (4)$$

where

$$iD_B(p) = \int_0^\infty \frac{ds}{\cos(eBs)} e^{is[p_\parallel^2 - p_\perp^2(\tan(eBs)/eBs) - m^2 + ie]} \quad (5)$$

and

$$\phi(x', x'') = \exp \left[ie \int_{x''}^{x'} dx_\mu A^\mu(x) \right]. \quad (6)$$

As the phase factor of the Schwinger's propagator is independent of the path, the overall phase of the one-loop self-energy involving two scalar particles becomes unity. Thus we can work in momentum space representation of the scalar propagator as given in Eq. (5). In this paper, we use the following convention: $g^{\mu\nu}$ is decomposed into two parts as $g^{\mu\nu} = g_{\parallel}^{\mu\nu} - g_{\perp}^{\mu\nu}$, where $g_{\parallel}^{\mu\nu} = \text{diag}(1, 0, 0, -1)$ and $g_{\perp}^{\mu\nu} = \text{diag}(0, 1, 1, 0)$. Similarly a general four vector can be written as $q^\mu = q_{\parallel}^\mu + q_{\perp}^\mu$ with $q_{\parallel}^2 = q_0^2 - q_3^2$ and $q_{\perp}^2 = q_1^2 + q_2^2$. Natural units will be used throughout the paper. From now on, the $i\epsilon$ term in the propagator will not be explicitly written and will be taken care of at the end of the calculation. The exact propagator in the external magnetic field can be written as a series in powers of eB [26]. As we are interested in the weak field regime, keeping only the lowest order terms we get

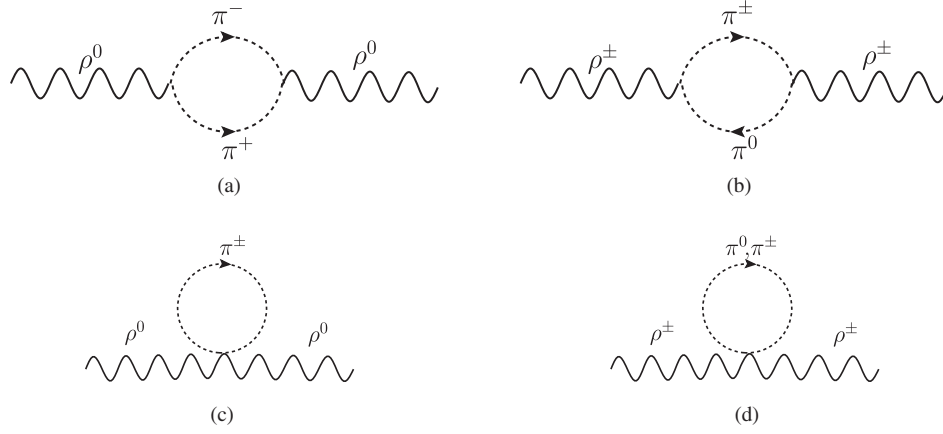
$$iD_B(p) \xrightarrow{eB \rightarrow 0} \frac{i}{p_\parallel^2 - p_\perp^2 - m^2} \\ \times \left[1 - \frac{(eB)^2}{(p_\parallel^2 - p_\perp^2 - m^2)^2} - \frac{2(eB)^2 p_\perp^2}{(p_\parallel^2 - p_\perp^2 - m^2)^3} \right]. \quad (7)$$

The phenomenological Lagrangian corresponding to $\rho\pi\pi$ interaction can be written as [28]

$$\mathcal{L}_{\rho\pi\pi} = -g_{\rho\pi\pi} \boldsymbol{\rho}^\mu \cdot (\boldsymbol{\pi} \times \partial_\mu \boldsymbol{\pi}) \\ + \frac{1}{2} g_{\rho\pi\pi}^2 (\boldsymbol{\rho}^\mu \times \boldsymbol{\pi}) \cdot (\boldsymbol{\rho}_\mu \times \boldsymbol{\pi}), \quad (8)$$

where the boldfaced ρ and π indicate that they are isovectors. Expanding the Lagrangian with complex pseudoscalar and vector fields, one can easily get the possible one-loop self-energy diagrams as shown in Fig. 1. In the following calculation we ignore the mass difference between neutral π meson and the charged π and denote the pion mass as m_π . Sometimes the superscript indices denoting neutral and charged ρ will be written downstairs for aesthetic reasons.

The part of the interaction Lagrangian which is responsible for the neutral ρ meson self-energy can be explicitly written as

FIG. 1. Feynman diagrams for the one-loop self-energy of ρ .

$$\mathcal{L}_{\rho_0} = ig_{\rho\pi\pi}[\rho_0^\mu(-\pi^-\partial_\mu\pi^+ + \partial_\mu\pi^-\pi^+)] + g_{\rho\pi\pi}^2\rho_0^2\pi^-\pi^+, \quad (9)$$

from which one can find the vertex factor for subdiagram (a) to be $\Gamma_a^\mu = -ig_{\rho\pi\pi}(2p+k)^\mu$ and that for subdiagram (c) to be $\Gamma_c = i2!g_{\rho\pi\pi}^2$. One loop self-energy for the ρ_0 meson is given by

$$-i\Pi_{\rho_0}^{\mu\nu} = \int \frac{d^4p}{(2\pi)^4} [\Gamma_a^\mu iD_B(p+k)\Gamma_a^\nu iD_B(p) + g^{\mu\nu}\Gamma_c iD_B(p)]$$

$$\Pi_{\rho_0}^{\mu\nu} = ig_{\rho\pi\pi}^2 \int \frac{d^4p}{(2\pi)^4} [(2p+k)^\mu(2p+k)^\nu D_B(p+k)D_B(p) - 2g^{\mu\nu}D_B(p)], \quad (10)$$

where

$$\Pi_{\rho_0}^{\mu\nu}(eB=0) = -\left(g^{\mu\nu} - \frac{k^\mu k^\nu}{k^2}\right)\Pi_{\text{vac}}(k^2)$$

$$\text{with } \Pi_{\text{vac}}(k^2) = \frac{1}{3} \frac{g_{\rho\pi\pi}^2}{16\pi^2} k^2 \left[\left(1 - \frac{4m_\pi^2}{k^2}\right)^{\frac{3}{2}} \ln\left(\frac{\sqrt{1 - 4m_\pi^2/k^2} + 1}{\sqrt{1 - 4m_\pi^2/k^2} - 1}\right) + \frac{8m_\pi^2}{k^2} + K \right], \quad (13)$$

where K contains the mass scale and can be fixed by an additional condition based on physical grounds. Although K is a constant in the case of pure vacuum, however in the presence of a magnetic field, the additional condition makes it in principle a function of eB as will be discussed in the next section. We denote the renormalized mass of the ρ meson as m_ρ whereas the magnetic field dependent effective mass is denoted as m_ρ^* .

In this work we are mainly concerned with the eB dependent one-loop self-energy up to $\mathcal{O}((eB)^2)$ which is reasonable in the weak field regime. After plugging in the propagators explicitly, the expression for the magnetic field dependent part of the neutral ρ meson self-energy becomes

$$\Pi_{\rho_0}^{\mu\nu}(eB \neq 0) = -i(eB)^2 g_{\rho\pi\pi}^2 \int \frac{d^4p}{(2\pi)^4} \left[(2p+k)^\mu(2p+k)^\nu \right.$$

$$\left. \times \left\{ \frac{p_\parallel^2 + p_\perp^2 - m_\pi^2}{[p^2 - m_\pi^2]^4 [(p+k)^2 - m_\pi^2]} + \frac{(p+k)_\parallel^2 + (p+k)_\perp^2 - m_\pi^2}{[p^2 - m_\pi^2][(p+k)^2 - m_\pi^2]^4} \right\} - 2g^{\mu\nu} \frac{p_\parallel^2 + p_\perp^2 - m_\pi^2}{(p^2 - m_\pi^2)^4} \right]. \quad (14)$$

$$D_B(p) = D_0(p) - (eB)^2 \frac{p_\parallel^2 + p_\perp^2 - m_\pi^2}{(p^2 - m_\pi^2)^4}, \quad (11)$$

and $D_0(p) = [p^2 - m_\pi^2]^{-1}$ is the free scalar propagator.

It is to be noted here that, as the vacuum part and the magnetic correction term of the propagator are additive, the one-loop self-energy of ρ_0 can be decomposed into two parts as

$$\Pi_{\rho_0}^{\mu\nu} = \Pi_{\rho_0}^{\mu\nu}(eB=0) + \Pi_{\rho_0}^{\mu\nu}(eB \neq 0). \quad (12)$$

This is true for the charged ρ mesons as well. After dimensional regularization and renormalization, the vacuum part of the self-energy which is finite and scale dependent can be written as [29,30]

Thus, we have altogether three integrals. The standard Feynman parametrization technique can be applied to these integrals one by one. Starting with the first one we find

$$\begin{aligned}
& \int \frac{d^4 p}{(2\pi)^4} (2p+k)^\mu (2p+k)^\nu \frac{p_\parallel^2 + p_\perp^2 - m_\pi^2}{[p^2 - m_\pi^2]^4 [(p+k)^2 - m_\pi^2]} \\
&= \int_0^1 dx 4(1-x)^3 \int \frac{d^4 p}{(2\pi)^4} \frac{1}{(p^2 - \Delta)^5} \\
&\quad \times [4[p_\parallel^\mu p_\parallel^\nu + p_\perp^\mu p_\perp^\nu][p_\parallel^2 + p_\perp^2 + x^2(k_\parallel^2 + k_\perp^2)] + (2x-1)^2 k^\mu k^\nu [p_\parallel^2 + p_\perp^2 + x^2(k_\parallel^2 + k_\perp^2)]] \\
&\quad + 4x(2x-1)[k^\mu \{p_\parallel^\nu (p_\parallel \cdot k_\parallel) - p_\perp^\nu (p_\perp \cdot k_\perp)\} + k^\nu \{p_\parallel^\mu (p_\parallel \cdot k_\parallel) - p_\perp^\mu (p_\perp \cdot k_\perp)\}] \\
&\quad - m_\pi^2 [4p^\mu p^\nu + (2x-1)^2 k^\mu k^\nu]. \tag{15}
\end{aligned}$$

It is worth mentioning that out of all the terms that emerge after the change of variable $p \rightarrow p - xk$, the bracketed terms are the only nonvanishing ones. Necessary identities for all the momentum integrations are given in the Appendix. Interestingly, one can skip the tenure of the calculation for the second integral by noticing that $p \leftrightarrow p + k$ transforms it exactly to the first one. Combining the contribution from the third integral with the first two, we find the following structure for the one-loop self-energy of the neutral ρ meson:

$$\begin{aligned}
\Pi_{\rho^0}^{\mu\nu} &= \Pi_{\rho^0}^{\mu\nu}(eB=0) + A_0 k^\mu k^\nu + B_0 g^{\mu\nu} + C_0 g_\perp^{\mu\nu} \\
&\quad + D_0 (k^\mu k_\perp^\nu + k^\nu k_\perp^\mu) \tag{16}
\end{aligned}$$

with the structure functions given as follows:

$$\begin{aligned}
A_0 &= \frac{2}{3} \frac{g_{\rho\pi\pi}^2 (eB)^2}{16\pi^2} \int_0^1 dx (1-x)^3 (1-2x) \\
&\quad \times \left[\left(\frac{(1-2x)(m_\pi^2 - 2k_\perp^2 x^2 - x^2 k^2)}{\Delta^3} \right) - \frac{2x}{\Delta^2} \right] \tag{17}
\end{aligned}$$

$$\begin{aligned}
B_0 &= \frac{1}{3} \frac{g_{\rho\pi\pi}^2 (eB)^2}{16\pi^2} \left[\frac{1}{m_\pi^2} - \int_0^1 dx (1-x)^3 \right. \\
&\quad \left. \times 2 \left(\frac{1}{\Delta} + \frac{m_\pi^2 - 2k_\perp^2 x^2 - x^2 k^2}{\Delta^2} \right) \right] \tag{18}
\end{aligned}$$

$$C_0 = -\frac{4}{3} \frac{g_{\rho\pi\pi}^2 (eB)^2}{16\pi^2} \int_0^1 dx \left[\frac{(1-x)^3}{\Delta} \right] \tag{19}$$

$$D_0 = \frac{4}{3} \frac{g_{\rho\pi\pi}^2 (eB)^2}{16\pi^2} \int_0^1 dx \left[\frac{x(1-x)^3(1-2x)}{\Delta} \right], \tag{20}$$

where $\Delta = x(x-1)k^2 + m_\pi^2 - i\epsilon$. Note the $i\epsilon$ term in the expression which takes into account its presence in all the Feynman propagators, not explicitly mentioned earlier. In a certain kinematic domain (like $k^2 \geq 4m_\pi^2$ where the unitary cut begins), the structure constants can have significant real and imaginary parts.

In the case of ρ^\pm mesons the contributing interaction Lagrangian is given by

$$\mathcal{L}_{\rho^\pm} = \rho_\mu^\pm (\pm \pi^\mp \partial^\mu \pi_0 \mp \pi^0 \partial^\mu \pi^\mp) + g_{\rho\pi\pi}^2 \rho^- (\pi_0^2 + \pi^- \pi^+) \rho^+.$$

Following a similar procedure, the magnetic field dependent self-energy of ρ^\pm up to $\mathcal{O}(eB)^2$ can be written as

$$\begin{aligned}
\Pi_{\rho^\pm}^{\mu\nu} &= i g_{\rho\pi\pi}^2 \int \frac{d^4 p}{(2\pi)^4} [(2p+k)^\mu (2p+k)^\nu D_B(p) D_0(p+k) - g^{\mu\nu} (2D_0(p) + 2D_B(p))] \\
&= -i (eB)^2 g_{\rho\pi\pi}^2 \int \frac{d^4 p}{(2\pi)^4} \left[(2p+k)^\mu (2p+k)^\nu \frac{p_\parallel^2 + p_\perp^2 - m_\pi^2}{[p^2 - m_\pi^2]^4 [(p+k)^2 - m_\pi^2]} - g^{\mu\nu} \frac{p_\parallel^2 + p_\perp^2 - m_\pi^2}{(p^2 - m_\pi^2)^4} \right]. \tag{21}
\end{aligned}$$

From this structure one can straightforwardly conclude that

$$\begin{aligned}
\Pi_{\rho^\pm}^{\mu\nu} &= \Pi_{\rho^\pm}^{\mu\nu}(eB=0) + A_\pm k^\mu k^\nu + B_\pm g^{\mu\nu} \\
&\quad + C_\pm g_\perp^{\mu\nu} + D_\pm (k^\mu k_\perp^\nu + k^\nu k_\perp^\mu), \tag{22}
\end{aligned}$$

where structure functions A_\pm, B_\pm, C_\pm, D are nothing but half of the A_0, B_0, C_0 and D_0 respectively.

The decay width of $\rho \rightarrow \pi\pi$ in the presence of a magnetic field is related to the imaginary part of the self-energy as [30]

$$\Gamma_\rho(eB) = \frac{\text{Im}\Pi(k_0 = m^*, eB)}{m^*}, \quad (23)$$

where Γ_ρ is defined in the rest frame of ρ with $\Pi = \frac{1}{3}\Pi_\mu^\mu$ and m^* is the solution of the equation

$$m^{*2} - m_\rho^2 + \text{Re}\Pi(k_0 = m^*, eB) = 0. \quad (24)$$

For a given value of eB , m^* gives the maximum of the spectral function which is defined as

$$\rho(k_0, eB) = \frac{\text{Im}\Pi}{(k_0^2 - m_\rho^2 + \text{Re}\Pi)^2 + (\text{Im}\Pi)^2}. \quad (25)$$

Note that, being a function of both $\text{Re}\Pi$ and $\text{Im}\Pi$ it carries all the essential features of the self-energy.

III. RESULTS

In this section we present the numerical results for the variation of the effective mass with weak external magnetic field. We consider the strength of the external field to be much less than the square of the ρ meson mass, i.e. $eB \ll m_\rho^2$. In our numerical calculation, we have taken the coupling constant $g_{\rho\pi\pi}$ as 6.03 which can be obtained by using the decay width of $\rho \rightarrow \pi\pi$ as 150 MeV. The mass of the pion is taken as 0.14 GeV. To get the effective mass numerically, we set the external three momentum of Eq. (3) to zero and obtain four mass relations given by

$$-m_\rho^2 + Ak_0^2 + B = 0 \quad (26)$$

$$k_0^2 - m_\rho^2 - \Pi_{\text{vac}}(k_0^2) + B - C = 0 \quad (27)$$

$$k_0^2 - m_\rho^2 - \Pi_{\text{vac}}(k_0^2) + B - C = 0 \quad (28)$$

$$k_0^2 - m_\rho^2 - \Pi_{\text{vac}}(k_0^2) + B = 0. \quad (29)$$

It must be noted here that for a given value of the parameter eB each of the equations possesses two unknowns, k_0 and the scale hidden in Π_{vac} . It might seem that the scale is already fixed by the condition employed at $eB = 0$ which is $\text{Re}\Pi_{\text{vac}}(k^2 = m_\rho^2) = 0$. But the physical mass in the presence of a magnetic field is m_ρ^* and not the vacuum mass m_ρ . Thus we must choose a more general condition $\text{Re}\Pi_{\text{vac}}(k^2 = m_\rho^{*2}) = 0$ which correctly reproduces the vacuum results in the absence of eB . Using the above condition we get the following mass relations:

$$-m_\rho^2 + Am_\rho^{*2} + B = 0 \quad (30)$$

$$m_\rho^{*2} - m_\rho^2 + B - C = 0 \quad (31)$$

$$m_\rho^{*2} - m_\rho^2 + B - C = 0 \quad (32)$$

$$m_\rho^{*2} - m_\rho^2 + B = 0, \quad (33)$$

where the subscripts of A , B , C and m_ρ^* are chosen accordingly. Out of the four relations, the first one gives an unphysical mode whereas the second and third one being same, are denoted as mode-1 with the last one denoted as mode-2. In both of the cases, we find that the effective mass of ρ^0 as well as ρ^\pm decreases with eB as shown in Fig. 2. To understand the connection between the modes and the spin states explicitly, one should note that, in the rest frame of a massive vector particle, the completeness relation satisfied by the polarization vectors is given as

$$\sum_{s=1}^3 \epsilon_s^\mu \epsilon_s^{*\nu} = -g^{\mu\nu} + u^\mu u^\nu, \quad (34)$$

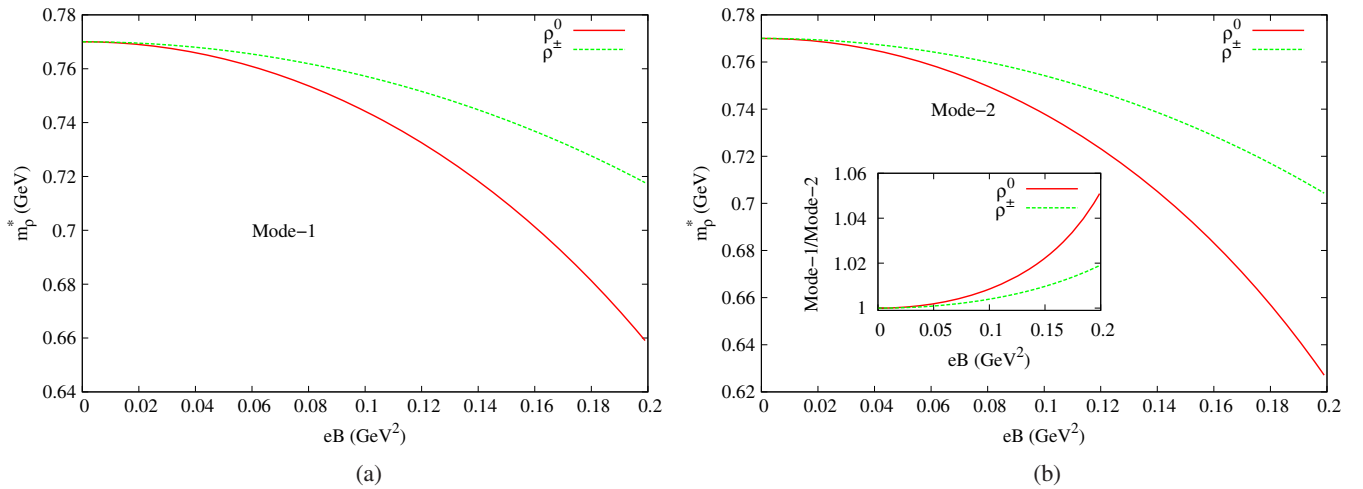


FIG. 2. Effective mass variations for $\rho\pi\pi$ coupling as a function of eB . Both of the modes show a decrease in effective mass of ρ^0 and ρ^\pm with the increasing external field. The ratio plotted in the inset demonstrates the difference between the two modes.

where

$$\begin{aligned}\epsilon_1^\mu(\mathbf{k}) &= \frac{1}{\sqrt{2}}(0, 1, i, 0) \\ \epsilon_2^\mu(\mathbf{k}) &= \frac{1}{\sqrt{2}}(0, 1, -i, 0) \\ \epsilon_3^\mu(\mathbf{k}) &= (0, 0, 0, 1) \\ u^\mu &= (1, 0, 0, 0).\end{aligned}\quad (35)$$

Using the completeness relation, the self-energy function in Eq. (16) can be decomposed in terms of the projection operators $P_s^{\mu\nu} = -\epsilon_s^\mu \epsilon_s^{*\nu}$ and $u^\mu u^\nu$. Inverting Eq. (1) one gets the one-loop corrected propagator as

$$\begin{aligned}D^{\mu\nu} &= \frac{P_1^{\mu\nu}}{k_0^2 - m_\rho^2 - \Pi_{\text{vac}}(k_0^2) + B - C} \\ &+ \frac{P_2^{\mu\nu}}{k_0^2 - m_\rho^2 - \Pi_{\text{vac}}(k_0^2) + B - C} \\ &+ \frac{P_3^{\mu\nu}}{k_0^2 - m_\rho^2 - \Pi_{\text{vac}}(k_0^2) + B} \\ &+ \frac{u^\mu u^\nu}{-m_\rho^2 + Ak_0^2 + B}.\end{aligned}\quad (36)$$

This form of the propagator simply indicates that mode-1 physically represents the spin state $S_z = \pm 1$ whereas $S_z = 0$ is represented by mode-2.

Although we started with the same physical mass for both ρ^0 and ρ^\pm which is 770 MeV, in both modes, their effective masses vary differently showing faster decrease for $m_{\rho^0}^*$ compared to $m_{\rho^\pm}^*$. However, if we compare the variations in the two modes by plotting the ratio of the effective masses as a function of eB (shown in the inset), we observe a difference between them which is in fact

relatively more prominent in the case of ρ^0 . The decreasing nature indicates the possibility of ρ condensation for higher magnetic fields. It also indicates that the critical field for ρ^0 meson should be smaller in magnitude compared to that for charged ρ . However, as we are working in the weak field regime, the prediction about the critical field eB_c is beyond the scope of our approximation. It is to be noted here that we find a nonzero effective mass for ρ^\pm even at $eB = 0.2 \text{ GeV}^2$ which differs from that predicted in Ref. [22]. Comparing with lattice results in Ref. [31], we find that our results agree in the case of ρ^0 with $S_z = 0$, ρ^+ with $S_z = +1$ and ρ^- with $S_z = -1$. These are the states for which ρ mass decreases with the magnetic field. In the rest of the cases, increase in eB also increases the mass.

In the case of dispersion relations, without any loss of generality we can reorient our axes such that $k_\perp^\mu = (0, k^1, k^2, 0)$ becomes $k_\perp^\mu = (0, 0, k_{\text{per}}, 0)$. Now, fixing the value of one of the independent variables in $k^\mu = (\omega, 0, k_{\text{per}}, k_z)$, we can find the variation of ω with respect to the other. In Fig. 3 the first column shows the variation of ω as a function of k_z with $k_{\text{per}} = 0.3 \text{ GeV}$. The mode energy increases with the increase of longitudinal momentum in all three modes tending to coincide with the vacuum for higher k_z values. This behavior is plausible because, for $k_z \gg eB$ the magnetic corrections do not contribute significantly resulting in lightlike dispersion. Similar behavior can be observed from the second column where k_{per} is varied keeping the longitudinal momentum fixed at 0.3 GeV. With the increase of eB from 0.1 to 0.2 GeV^2 , one can notice the downward shift of the dispersion curves in all three modes.

To calculate the decay width and spectral function in the rest frame of ρ , we need to know the imaginary parts of A , B and C . The imaginary parts of those structure functions can be obtained analytically and are given as follows:

$$\begin{aligned}\frac{1}{2} \text{Im}[A] &= -\frac{\pi}{2} \left[\frac{96m_\pi^4}{(k_0^2)^{5/2}(k_0^2 - 4m_\pi^2)^{3/2}} - \frac{32m_\pi^2}{(k_0^2)^{3/2}(k_0^2 - 4m_\pi^2)^{3/2}} \right. \\ &\quad \left. + \frac{2}{\sqrt{k_0^2}(k_0^2 - 4m_\pi^2)^{3/2}} + \frac{24m_\pi^2}{(k_0^2)^{5/2}\sqrt{k_0^2 - 4m_\pi^2}} - \frac{4}{(k_0^2)^{3/2}\sqrt{k_0^2 - 4m_\pi^2}} \right] (eB)^2\end{aligned}\quad (37)$$

$$-\frac{1}{2} \text{Im}[B] = -\frac{\pi}{2} \left[\frac{24m_\pi^4}{(k_0^2)^{3/2}(k_0^2 - 4m_\pi^2)^{3/2}} - \frac{6m_\pi^2}{\sqrt{k_0^2}(k_0^2 - 4m_\pi^2)^{3/2}} + \frac{12\frac{m_\pi^2}{k_0} - 4}{2\sqrt{k_0^2}\sqrt{k_0^2 - 4m_\pi^2}} \right] (eB)^2\quad (38)$$

$$-\frac{1}{4} \text{Im}[C] = -\frac{\pi}{2} \left[\frac{12\frac{m_\pi^2}{k_0} - 4}{2\sqrt{k_0^2}\sqrt{k_0^2 - 4m_\pi^2}} \right] (eB)^2,\quad (39)$$

where the expressions are scaled by the overall common factor $g_{\rho\pi\pi}^2/48\pi^2$ for ρ^0 and half of that for ρ^\pm . Using the definition given in Eq. (23) we obtain the decay width for

$\rho \rightarrow \pi\pi$ as shown in the left panel of Fig. 4. It has been found that Γ_ρ decreases with the external magnetic field both for ρ^0 and ρ^\pm . However, the rate of decrease being

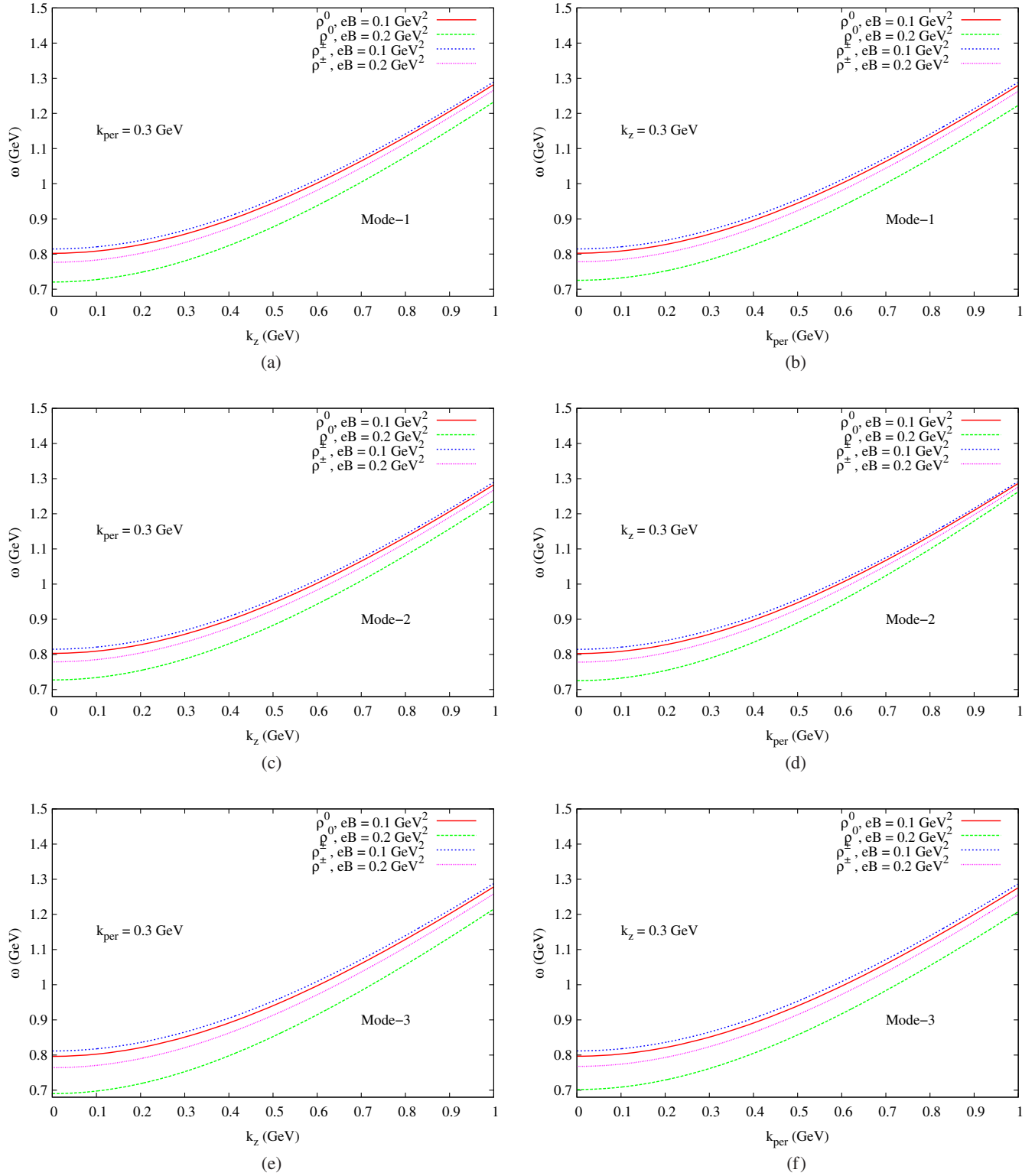


FIG. 3. Dispersion relations of ρ^0 and ρ^\pm for two different values of eB in the weak field regime. The left panel shows the variation with k_z for a fixed value of k_{per} . The right panel instead shows the dispersion as a function of k_{per} keeping the k_z fixed.

small, it never vanishes even for $eB = 0.2 \text{ GeV}^2$ which we have taken to be the maximum limit of the external field as mentioned earlier. The fact indicates that, in the weak field limit, there exists suppression in the decay channel of

$\rho \rightarrow \pi\pi$ but the prediction for complete blockage of the channel is beyond the scope of its applicability.

Spectral functions are plotted in the right panel with two nonzero values of eB . As soon as the magnetic field is

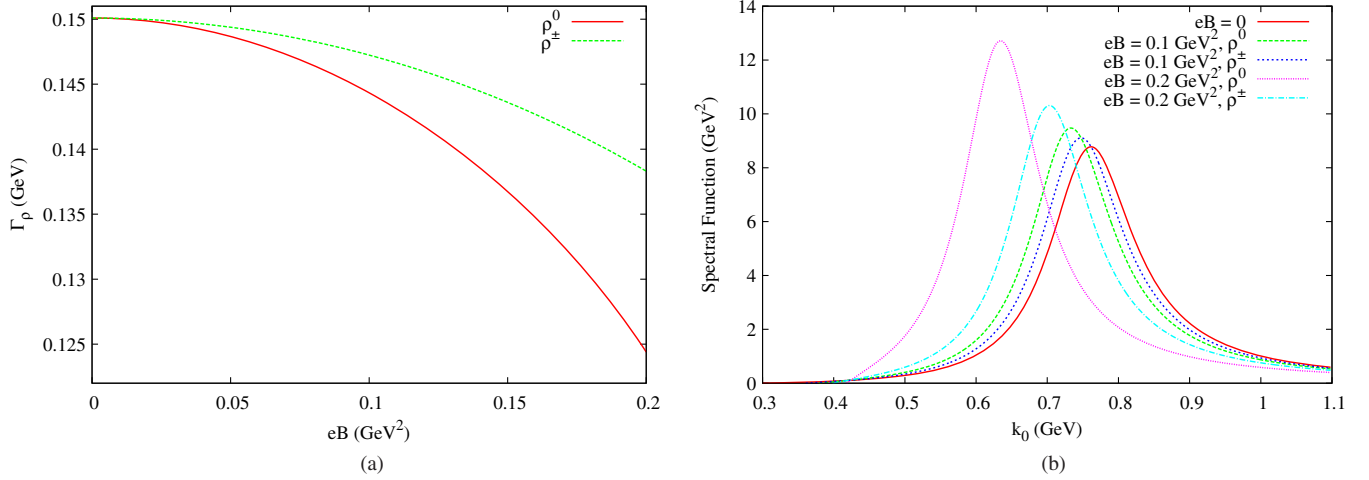


FIG. 4. The left panel shows the variation of decay width of ρ mesons with external magnetic field. Γ_ρ for both ρ^0 and ρ^\pm decreases with magnetic field but remains finite even at a maximum value of $eB = 0.2 \text{ GeV}^2$. Spectral functions are plotted in the right panel for $eB = \{0, 0.1, 0.2\} \text{ GeV}^2$. It becomes narrower and taller as it shifts towards the lower values of k_0 .

turned on, the vacuum spectral function splits into two, corresponding to different self-energies of ρ^0 and ρ^\pm . It is the interplay between k_0 and eB dependencies of $\text{Im}\Pi$ which makes the spectral function narrower and taller as it shifts towards the condensation. The shift is the manifestation of decreasing m^* which is the k_0 value corresponding to the maximum of the spectral function. These features of the spectral function are consistent with the qualitative discussions given in [8]. However, unlike [8], the shift for ρ^0 in our case is more in comparison with that of ρ^\pm which is expected from our results of m_{ρ^*} and Γ_ρ .

IV. SUMMARY AND CONCLUSIONS

In this paper, we have investigated the charged and neutral ρ meson condensation in the external magnetic field. We restricted ourselves to the weak field regime and used the series form of the scalar propagator in the magnetic background taking into consideration the leading order magnetic correction term. Starting from the phenomenological Lagrangian, we explicitly calculated the magnetic correction to the one-loop self-energy up to $\mathcal{O}(eB)^2$. Using the standard Dyson-Schwinger equation, we have calculated the effective mass variations for ρ^0 and ρ^\pm . In this case we find two independent physical modes both of them showing decreasing nature which indicates the possibility of ρ condensation. However, because of our restriction to the weak field regime, we cannot predict the exact value of critical field at which the effective mass vanishes but we do find nonzero $m_{\rho^\pm}^*$ for $eB = 0.2 \text{ GeV}$. The trend shows that the critical field for the ρ meson (both ρ^0 and ρ^\pm) will be higher than the prediction made in [22]. Moreover, in our case ρ^0 mass falls faster than ρ^\pm with increasing B which differs from the result of Liu *et al.* [22]. In addition to that we have also presented the modified

dispersion relations of the ρ meson for three distinct modes. The imaginary parts of the structure functions have been obtained analytically. We have also explicitly calculated the spectral function for the first time. The shift in the spectral function with the increasing magnetic field is in agreement with what has been anticipated in [8] based on qualitative arguments. Another important difference of our work in comparison with that of Ref. [22] is that, in the NJL model, the quarks are affected by the magnetic field. That means the magnetically corrected propagators appearing in the self-energy should be fermionic propagators. But in our case, pionic fields contribute to the ρ self-energy. Thus bosonic propagators contain the magnetic corrections. Now, the essential difference between the two is that in weak field expansion, fermionic propagators possess corrections of eB order [32] but in the case of bosons, the leading order correction is $\mathcal{O}((eB)^2)$ [26]. Thus, one can expect that no eB order correction can be introduced with it. It is true that depending upon the interactions, even if one uses $\mathcal{O}(eB)$ corrected fermionic propagators, the leading order contribution to self-energy may not be of $\mathcal{O}(eB)$ [24]. However, the discussions in [22] clearly indicate that at least in the case of m_{ρ^\pm} with $S_z = \pm 1$, the magnetic correction of $\mathcal{O}(eB)$ exists and it is the only mode for which a decrease in mass has been observed. Our spin decomposition in the rest frame is similar to that of [22]. We are also not considering the lowest Landau level (LLL) approximation. Thus we find that the possibility of observation of ρ meson condensation in the weak magnetic field depends upon the interaction terms used in the Lagrangian and undoubtedly demands further investigation.

At this point it is necessary to mention that our phenomenological Lagrangian considers only the $\rho\pi\pi$ interaction which takes into account, in fact, the largest decay channel (~ 100 percent) of rho meson which is

$\rho \rightarrow \pi\pi$. Nevertheless, because of its simplicity, our phenomenological Lagrangian can be implemented at finite temperature calculations as well, which will be discussed elsewhere [25].

ACKNOWLEDGMENT

S. G. acknowledges Centre for Nuclear Theory, Department of Atomic Energy for support.

APPENDIX: USEFUL IDENTITIES

Here we list all the identities necessary to perform the momentum integrations of Eq. (15). All through the section we use $\Delta = x(x-1)k^2 + m_\pi^2$.

Identity 1:

$$\begin{aligned} \int \frac{d^4 p}{(2\pi)^4} \frac{1}{(p^2 - \Delta)^5} &= -i \frac{1}{(4\pi)^2} \frac{1}{(\Delta)^3} \frac{\Gamma[3]}{\Gamma[5]} \\ &= -\frac{i}{12} \frac{1}{(4\pi)^2} \frac{1}{\Delta^3}. \end{aligned} \quad (\text{A1})$$

Identity 2:

$$\begin{aligned} \int \frac{d^4 p}{(2\pi)^4} \frac{p^\mu p^\nu}{(p^2 - \Delta)^5} &= \frac{g^{\mu\nu}}{4} \int \frac{d^4 p}{(2\pi)^4} \frac{p^2}{(p^2 - \Delta)^5} \\ &= \frac{g^{\mu\nu}}{4} \frac{i}{(4\pi)^2} \frac{1}{(\Delta)^2} \frac{\Gamma[3]}{\Gamma[5]} \\ &= \frac{i}{48} \frac{1}{(4\pi)^2} \frac{1}{(\Delta)^2} g^{\mu\nu}. \end{aligned} \quad (\text{A2})$$

Identity 3:

$$\begin{aligned} \int \frac{d^4 p}{(2\pi)^4} \frac{p_\parallel^2}{(p^2 - \Delta)^5} &= i \int \frac{d^2 p_\perp}{(2\pi)^2} \int \frac{d^2 p_{E_\parallel}}{(2\pi)^2} \frac{p_{E_\parallel}^2}{(p_{E_\parallel}^2 + \Delta_\parallel)^5} \\ &= i \frac{1}{4\pi} \int \frac{d^2 p_\perp}{(2\pi)^2} \frac{1}{(p_\perp^2 + \Delta)^3} \frac{\Gamma[3]}{\Gamma[5]} \\ &= i \frac{1}{(4\pi)^2} \frac{1}{\Delta^2} \frac{\Gamma[2]}{\Gamma[3]} \frac{\Gamma[3]}{\Gamma[5]} \\ &= \frac{i}{24} \frac{1}{(4\pi)^2} \frac{1}{\Delta^2}. \end{aligned} \quad (\text{A3})$$

Identity 4:

$$\begin{aligned} \int \frac{d^4 p}{(2\pi)^4} \frac{p_\perp^2}{(p^2 - \Delta)^5} &= -i \int \frac{d^2 p_\perp}{(2\pi)^2} p_\perp^2 \int \frac{d^2 p_{E_\parallel}}{(2\pi)^2} \frac{1}{(p_{E_\parallel}^2 + \Delta_\parallel)^5} \\ &= -\frac{i}{4\pi} \int \frac{d^2 p_\perp}{(2\pi)^2} p_\perp^2 \frac{1}{(p_\perp^2 + \Delta)^4} \frac{\Gamma[4]}{\Gamma[5]} \\ &= -\frac{i}{(4\pi)^2} \frac{1}{\Delta^2} \frac{\Gamma[4]}{\Gamma[4]} \frac{\Gamma[4]}{\Gamma[5]} \\ &= -\frac{i}{24} \frac{1}{(4\pi)^2} \frac{1}{\Delta^2}. \end{aligned} \quad (\text{A4})$$

Identity 5:

$$\begin{aligned} \int \frac{d^4 p}{(2\pi)^4} \frac{p_\parallel^\mu p_\parallel^\nu}{(p^2 - \Delta)^5} &= \frac{g_\parallel^{\mu\nu}}{2} \int \frac{d^4 p}{(2\pi)^4} \frac{p_\parallel^2}{(p^2 - \Delta)^5} \\ &= g_\parallel^{\mu\nu} \frac{i}{48} \frac{1}{(4\pi)^2} \frac{1}{\Delta^2}. \end{aligned} \quad (\text{A5})$$

Identity 6:

$$\begin{aligned} \int \frac{d^4 p}{(2\pi)^4} \frac{p_\perp^\mu p_\perp^\nu}{(p^2 - \Delta)^5} &= \frac{g_\perp^{\mu\nu}}{2} \int \frac{d^4 p}{(2\pi)^4} \frac{p_\perp^2}{(p^2 - \Delta)^5} \\ &= -g_\perp^{\mu\nu} \frac{i}{48} \frac{1}{(4\pi)^2} \frac{1}{\Delta^2}. \end{aligned} \quad (\text{A6})$$

Identity 7:

$$\begin{aligned} \int \frac{d^4 p}{(2\pi)^4} \frac{p_\parallel^2 p_\parallel^\mu p_\parallel^\nu}{(p^2 - \Delta)^5} &= \frac{g_\parallel^{\mu\nu}}{2} \int \frac{d^4 p}{(2\pi)^4} \frac{p_\parallel^4}{(p^2 - \Delta)^5} \\ &= -i \frac{g_\parallel^{\mu\nu}}{2} \int \frac{d^2 p_\perp}{(2\pi)^2} \int \frac{d^2 p_{E_\parallel}}{(2\pi)^2} \frac{(p_{E_\parallel}^2)^2}{(p_{E_\parallel}^2 + \Delta_\parallel)^5} \\ &= -i \frac{g_\parallel^{\mu\nu}}{2} \int \frac{d^2 p_\perp}{(2\pi)^2} \frac{1}{4\pi} \frac{1}{(p_\perp^2 + \Delta)^2} \frac{\Gamma[3]}{\Gamma[5]} \\ &= -g_\parallel^{\mu\nu} \frac{i}{24} \frac{1}{(4\pi)^2} \frac{1}{\Delta}. \end{aligned} \quad (\text{A7})$$

Identity 8:

$$\begin{aligned}
\int \frac{d^4 p}{(2\pi)^4} \frac{p_\perp^2 p_\parallel^\mu p_\perp^\nu}{(p^2 - \Delta)^5} &= \frac{g_\parallel^{\mu\nu}}{2} \int \frac{d^4 p}{(2\pi)^4} \frac{p_\parallel^2 p_\perp^2}{(p^2 - \Delta)^5} \\
&= i \frac{g_\parallel^{\mu\nu}}{2} \int \frac{d^2 p_\perp}{(2\pi)^2} p_\perp^2 \int \frac{d^2 p_{E_\parallel}}{(2\pi)^2} \frac{p_{E_\parallel}^2}{(p_{E_\parallel}^2 + \Delta_\parallel)^5} \\
&= i \frac{g_\parallel^{\mu\nu}}{2} \int \frac{d^2 p_\perp}{(2\pi)^2} p_\perp^2 \frac{1}{4\pi} \frac{1}{(p_\perp^2 + \Delta)^3} \frac{\Gamma[3]}{\Gamma[5]} \\
&= i \frac{g_\parallel^{\mu\nu}}{2} \frac{1}{(4\pi)^2} \frac{1}{\Delta} \frac{\Gamma[3]}{\Gamma[5]} \\
&= g_\parallel^{\mu\nu} \frac{i}{48} \frac{1}{(4\pi)^2} \frac{1}{\Delta}. \tag{A8}
\end{aligned}$$

Identity 9:

$$\begin{aligned}
\int \frac{d^4 p}{(2\pi)^4} \frac{p_\parallel^2 p_\perp^\mu p_\perp^\nu}{(p^2 - \Delta)^5} &= \frac{g_\perp^{\mu\nu}}{2} \int \frac{d^4 p}{(2\pi)^4} \frac{p_\parallel^2 p_\perp^2}{(p^2 - \Delta)^5} \\
&= g_\perp^{\mu\nu} \frac{i}{48} \frac{1}{(4\pi)^2} \frac{1}{\Delta}. \tag{A9}
\end{aligned}$$

Identity 10:

$$\begin{aligned}
\int \frac{d^4 p}{(2\pi)^4} \frac{p_\perp^2 p_\perp^\mu p_\perp^\nu}{(p^2 - \Delta)^5} &= \frac{g_\perp^{\mu\nu}}{2} \int \frac{d^4 p}{(2\pi)^4} \frac{p_\perp^4}{(p^2 - \Delta)^5} \\
&= -i \frac{g_\perp^{\mu\nu}}{2} \int \frac{d^2 p_\perp}{(2\pi)^2} p_\perp^4 \int \frac{d^2 p_{E_\parallel}}{(2\pi)^2} \frac{1}{(p_{E_\parallel}^2 + \Delta_\parallel)^5} \\
&= -i \frac{g_\perp^{\mu\nu}}{2} \int \frac{d^2 p_\perp}{(2\pi)^2} p_\perp^4 \frac{1}{4\pi} \frac{1}{(p_\perp^2 + \Delta)^4} \frac{\Gamma[4]}{\Gamma[5]} \\
&= -i \frac{g_\perp^{\mu\nu}}{2} \frac{1}{(4\pi)^2} \frac{\Gamma[3]\Gamma[4]}{\Delta\Gamma[4]\Gamma[5]} \\
&= -g_\perp^{\mu\nu} \frac{i}{24} \frac{1}{(4\pi)^2} \frac{1}{\Delta}. \tag{A10}
\end{aligned}$$

Identity 11:

$$\int \frac{d^4 p}{(2\pi)^4} \frac{p_\parallel^\mu (p_\parallel \cdot k_\parallel)}{(p^2 - \Delta)^5} = \frac{i}{48} \frac{1}{(4\pi)^2} \frac{1}{\Delta^2} k_\parallel^\mu. \tag{A11}$$

Identity 12:

$$\int \frac{d^4 p}{(2\pi)^4} \frac{p_\perp^\mu (p_\perp \cdot k_\perp)}{(p^2 - \Delta)^5} = -\frac{i}{48} \frac{1}{(4\pi)^2} \frac{1}{\Delta^2} k_\perp^\mu. \tag{A12}$$

Identity 13:

$$\int \frac{d^4 p}{(2\pi)^4} \frac{p_\parallel^2}{(p^2 - m_\pi^2)^4} = -\frac{i}{(4\pi)^2} \frac{1}{6} \frac{1}{m_\pi^2}. \tag{A13}$$

Identity 14:

$$\int \frac{d^4 p}{(2\pi)^4} \frac{p_\perp^2}{(p^2 - m_\pi^2)^4} = \frac{i}{(4\pi)^2} \frac{1}{6} \frac{1}{m_\pi^2}. \tag{A14}$$

Identity 15:

$$\int \frac{d^4 p}{(2\pi)^4} \frac{1}{(p^2 - m_\pi^2)^4} = \frac{i}{(4\pi)^2} \frac{1}{6} \frac{1}{(m_\pi^2)^2}. \tag{A15}$$

-
- [1] D. E. Kharzeev, K. Landsteiner, A. Schmitt, and H. U. Yee, *Lect. Notes Phys.* **871**, 1 (2013).
[2] D. E. Kharzeev and A. Zhitnitsky, *Nucl. Phys.* **A797**, 67 (2007).
[3] D. E. Kharzeev, L. D. McLerran, and H. J. Warringa, *Nucl. Phys.* **A803**, 227 (2008).
[4] K. Fukushima, D. E. Kharzeev, and H. J. Warringa, *Phys. Rev. D* **78**, 074033 (2008).
[5] V. P. Gusynin, V. A. Miransky, and I. A. Shovkovy, *Nucl. Phys.* **B462**, 249 (1996); **563**, 361 (1999).
[6] G. S. Bali, F. Bruckmann, G. Endrodi, Z. Fodor, S. D. Katz, S. Kreig, A. Schafer, and K. K. Szabo, *J. High Energy Phys.* **02** (2012) 044.
[7] M. N. Chernodub, *Lect. Notes Phys.* **871**, 143 (2013).
[8] M. N. Chernodub, *Phys. Rev. D* **82**, 085011 (2010).
[9] M. N. Chernodub, *Phys. Rev. Lett.* **106**, 142003 (2011).
[10] V. Skokov, A. Y. Illarionov, and V. Toneev, *Int. J. Mod. Phys. A* **24**, 5925 (2009).
[11] R. C. Duncan and C. Thompson, *Astrophys. J.* **392**, L9 (1992).
[12] E. J. Ferrer, V. de la Incera, and C. Manuel, *Phys. Rev. Lett.* **95**, 152002 (2005); *Nucl. Phys.* **B747**, 88 (2006).
[13] E. J. Ferrer and V. de la Incera, *Phys. Rev. D* **76**, 045011 (2007).
[14] K. Fukushima and H. J. Warringa, *Phys. Rev. Lett.* **100**, 032007 (2008).
[15] B. Feng, D. Hou, H.-C. Ren, and P.-P. Wu, *Phys. Rev. Lett.* **105**, 042001 (2010).
[16] S. Fayazbakhsh and N. Sadooghi, *Phys. Rev. D* **82**, 045010 (2010); **83**, 025026 (2011).

- [17] C. Vafa and E. Witten, *Nucl. Phys.* **B234**, 173 (1984).
- [18] Y. Hidaka and A. Yamamoto, *Phys. Rev. D* **87**, 094502 (2013).
- [19] M. N. Chernodub, *Phys. Rev. D* **86**, 107703 (2012).
- [20] C. Li and Q. Wang, *Phys. Lett. B* **721**, 141 (2013).
- [21] M. N. Chernodub, *Phys. Rev. D* **89**, 018501 (2014).
- [22] H. Liu, L. Yu, and M. Huang, *Phys. Rev. D* **91**, 014017 (2015).
- [23] M. Kawaguchi and S. Matsuzaki, *Phys. Rev. D* **93**, 125027 (2016).
- [24] S. P. Adhya, M. Mandal, S. Biswas, and P. K. Roy, *Phys. Rev. D* **93**, 074033 (2016).
- [25] A. Mukherjee, S. Ghosh, M. Mandal, P. K. Roy, and S. Sarkar (to be published).
- [26] A. Ayla, A. Sánchez, G. Piccinelli, and S. Sahu, *Phys. Rev. D* **71**, 023004 (2005).
- [27] J. Schwinger, *Phys. Rev.* **82**, 664 (1951).
- [28] S. Sarkar, J. Alam, P. Roy, A. K. Dutt-Mazumder, B. Dutta-Roy, and B. Sinha, *Nucl. Phys.* **A634**, 206 (1998).
- [29] C. Quigg, *Gauge Theories of the Strong, Weak, and Electromagnetic Interactions* (Princeton University Press, Princeton, NJ, 2013).
- [30] C. Gale and J. I. Kapusta, *Nucl. Phys.* **B357**, 65 (1991).
- [31] E. V. Luschevskaya, O. A. Kochetkov, O. V. Larina, and O. V. Teryaev, *Proc. Sci. LATTICE2014* (2014) 120 [arXiv: 1411.0730v1]; E. V. Luschevskaya and O. V. Larina, *JETP Lett.* **98**, 652 (2014).
- [32] T. Chyi, C. Hwang, W. F. Kao, G. Lin, K. Ng, and J. Tseng, *Phys. Rev. D* **62**, 105014 (2000).